



# Comparison of the Electrochemical Performance and Thermal Stability for Three Kinds of Charged Cathodes

Guobin Zhong<sup>1</sup>, Jinqiu Gong<sup>2</sup>, Chao Wang<sup>1</sup>, Kaiqi Xu<sup>1</sup> and Haodong Chen<sup>2\*</sup>

<sup>1</sup> Electric Power Research Institute of Guangdong Power Grid Co., Ltd., Guangzhou, China, <sup>2</sup> Institute of Advanced Technology, University of Science and Technology of China, Hefei, China

## OPEN ACCESS

### Edited by:

Qingsong Wang,  
University of Science and Technology  
of China, China

### Reviewed by:

Yong Chen,  
Hainan University, China  
Huan Pang,  
Yangzhou University, China

### \*Correspondence:

Haodong Chen  
linghao@ustc.edu.cn

### Specialty section:

This article was submitted to  
Energy Storage,  
a section of the journal  
Frontiers in Energy Research

**Received:** 15 July 2018

**Accepted:** 02 October 2018

**Published:** 30 October 2018

### Citation:

Zhong G, Gong J, Wang C, Xu K and  
Chen H (2018) Comparison of the  
Electrochemical Performance and  
Thermal Stability for Three Kinds of  
Charged Cathodes.  
Front. Energy Res. 6:110.  
doi: 10.3389/fenrg.2018.00110

The electrochemical performance and thermal stability of  $\text{Li}(\text{Ni}_{0.5}\text{Co}_{0.2}\text{Mn}_{0.3})\text{O}_2$ ,  $\text{LiMn}_2\text{O}_4$ , and  $\text{LiFePO}_4$  are investigated by the multi-channel battery cycler, electrochemical workstation, thermogravimetric analysis (TGA) and C80 instrument in this work. For electrochemical performance,  $\text{Li}(\text{Ni}_{0.5}\text{Co}_{0.2}\text{Mn}_{0.3})\text{O}_2$  shows the highest specific capacity but the worst cycle stability. For the thermal stability, the experimental results of thermogravimetry and C80 indicate that the charged  $\text{Li}(\text{Ni}_{0.5}\text{Co}_{0.2}\text{Mn}_{0.3})\text{O}_2$  has the worst thermal stability compared with charged  $\text{LiFePO}_4$  and  $\text{LiMn}_2\text{O}_4$ . It is also testified by calculating the chemical kinetic parameters of cathode materials based on the Arrhenius law. The pure  $\text{Li}(\text{Ni}_{0.5}\text{Co}_{0.2}\text{Mn}_{0.3})\text{O}_2$  starts to self-decompose at around  $250^\circ\text{C}$  with total heat generation of  $-88\text{ J/g}$ . As for a full battery, the total heat generation is  $-810\text{ J/g}$  with exothermic peak temperature of  $242^\circ\text{C}$ . The present results show that thermal runaway is more likely to occur for  $\text{Li}(\text{Ni}_{0.5}\text{Co}_{0.2}\text{Mn}_{0.3})\text{O}_2$  with the full battery.

**Keywords:** lithium ion battery safety, cathode materials, electrochemical analysis, thermal analysis, thermal runaway

## INTRODUCTION

Lithium-ion batteries (LIBs) are widely used in a variety of areas for their high-energy density, such as portable telephones, computers and electric vehicles (EVs) (Sun et al., 2009; Hannan et al., 2017). However, the safety issue cannot be ignored because there are so many accidents for fires and explosions that occur frequently due to the potential hazard of batteries (Wang et al., 2012). Meanwhile, as an important part of battery, cathode materials such as  $\text{Li}(\text{Ni}_{0.5}\text{Co}_{0.2}\text{Mn}_{0.3})\text{O}_2$  (NCM523),  $\text{LiMn}_2\text{O}_4$  (LMO) and  $\text{LiFePO}_4$  (LFP) have received much attention recently. The characteristics of cost, performance and safety should be taken into consideration.

For  $\text{LiMn}_2\text{O}_4$  cathode material, it is cheap and with good thermal stability. Whereas  $\text{LiMn}_2\text{O}_4$  belongs to spinel-type structure with worse cycle performance, which is affected by Jahn-Teller distortion accompanied with structural transformation during charge-discharge process (Ouyang et al., 2009). A lots of work has been conducted to improve the performance of  $\text{LiMn}_2\text{O}_4$  by doping with diverse elements, such as F (Chen et al., 2010; Feng et al., 2010), Cr (Xu et al., 2011), Nb (Yi et al., 2013), Mg (Susanto et al., 2015).  $\text{LiFePO}_4$  is more stable but the conductivity is poor. Zaghbi

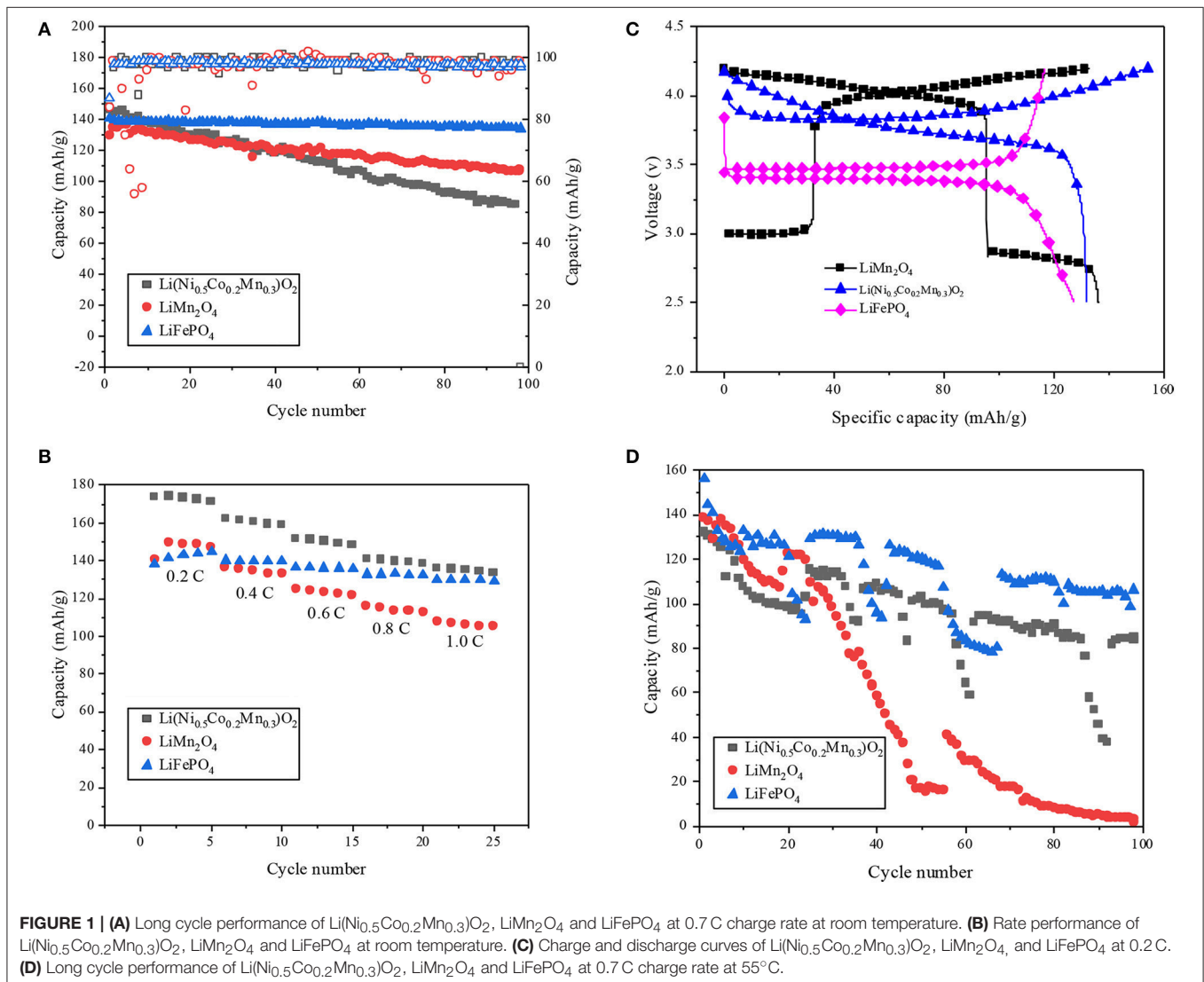
et al. enhanced the thermal safety and high power performance of  $\text{LiFePO}_4$  with coated carbon (Zaghib et al., 2012). While  $\text{Li}(\text{Ni}_{0.5}\text{Co}_{0.2}\text{Mn}_{0.3})\text{O}_2$  has high-energy density but fragile structural stability, some modifications have been made to improve the cycle performance and thermal stability, such as graphene oxide with  $\text{V}_2\text{O}_5$  coating (Luo and Zheng, 2017),  $\text{AlF}_3$  coating (Yang et al., 2012). Gong et al. analyzed the total exothermic heat of nickel cobalt lithium manganese with various nickel content and it increased as nickel content increased (Gong et al., 2017). In addition, Pang et al. reviewed the application of  $\text{MnO}$  (Chen et al., 2018),  $\text{FeO}_x$  (Ma et al., 2018), and  $\text{M}_x\text{S}_y$  ( $\text{M} = \text{Cu}, \text{Ag}, \text{Au}$ ) (Lu et al., 2017) in LIBs.

Although the improvement of these cathode materials has been investigated (Julien et al., 2014b; Du et al., 2016), however, an elaborate comparison of the electrochemical performance and thermal stability were rare reported in previous work. In this work, the electrochemical performance and thermal stability of charged  $\text{Li}(\text{Ni}_{0.5}\text{Co}_{0.2}\text{Mn}_{0.3})\text{O}_2$ ,  $\text{LiMn}_2\text{O}_4$  and  $\text{LiFePO}_4$  are analyzed and compared.

## EXPERIMENTAL

### Electrochemical Measurements

The positive electrodes contain commercial cathode materials including  $\text{Li}(\text{Ni}_{0.5}\text{Co}_{0.2}\text{Mn}_{0.3})\text{O}_2$ ,  $\text{LiMn}_2\text{O}_4$ , and  $\text{LiFePO}_4$ , acetylene black and polyvinylidene fluoride, and the mass ratio of the active material, acetylene black and polyvinylidene fluoride is 8:1:1. The commercial organic electrolyte with 1.0 M  $\text{LiPF}_6$  salt and the mixture solvent of ethylene carbonate (EC) and diethyl carbonate (DEC) (1:1, w:w) and the separator being made of Celgard 2,400 polyethylene were used. The CR2032 type coin half-cell was assembled in the glove box filled with argon atmosphere (SG2400/750TS, Vigor, Suzhou, China,  $\text{O}_2 < 1$  ppm,  $\text{H}_2\text{O} < 1$  ppm). Galvanostatic charge and discharge tests at 0.7 C were conducted on a multi-channel battery cycler (Neware, BTS-6V 10 mA, China) with the voltage range from 2.5 to 4.2 V at room temperature and  $55^\circ\text{C}$ , respectively. The AC impedance and cyclic voltammetry were measured by a CHI 604A electrochemical workstation.



## Thermal Analysis Methods

In order to evaluate the thermal stability of the cathode material in the most dangerous state of charge, the half-cell with the three kinds of cathode materials were pre-cycled three times and then fully charged to 4.2 V. After this, the fully charged cathode materials were disassembled in the argon atmosphere. The obtained cathodes were rinsed by dimethyl carbonate (DMC) solvent to defuse the residual electrolyte. The weight loss of materials was tested by a STA490C thermal analyzer at a heating/cooling rate of 10°C/min with 200 mL/min flow of N<sub>2</sub> in the temperature range of 30–800°C. The heat flow of the materials was measured by a C80 instrument filled with argon atmosphere at 0.2°C/min in the temperature range of room temperature to 300°C. The thermal effects of each sample were thus recorded automatically, and the C80 calculations were based on dry film weight of the electrode material.

## Characterization Analysis

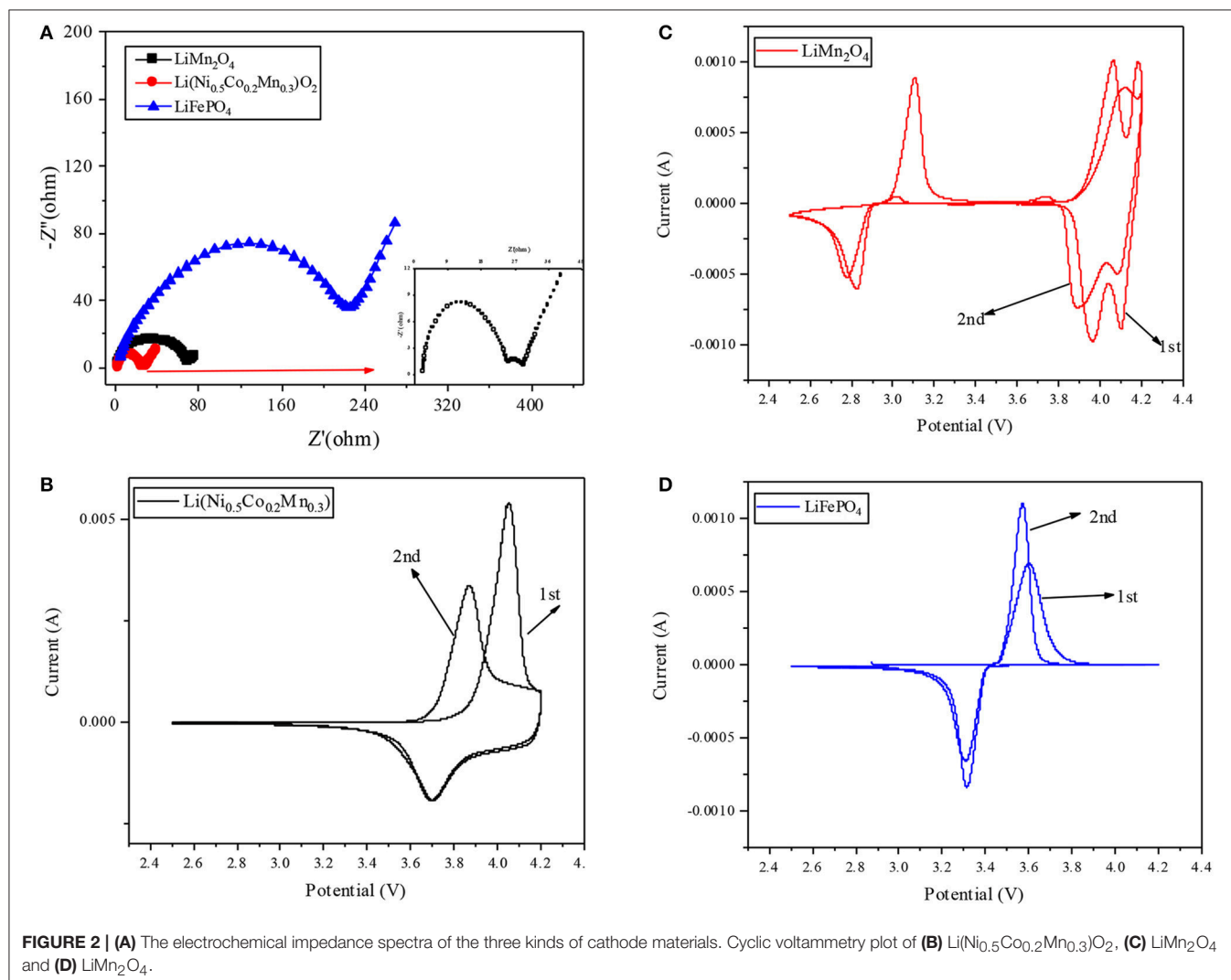
X-ray diffraction (XRD) (Cu K $\alpha$ , MXPAHF) information and scanning electron microscopy (SEM, FEI Sirion200) images of

Li(Ni<sub>0.5</sub>Co<sub>0.2</sub>Mn<sub>0.3</sub>)O<sub>2</sub>, LiMn<sub>2</sub>O<sub>4</sub>, and LiFePO<sub>4</sub> before and after thermal treatment were conducted.

## RESULTS AND DISCUSSION

### Comparison on Electrochemical Performance

**Figure 1A** shows the long cycle performance of the three kinds of cathode materials at 0.7 C charge rate. It can be seen that LiFePO<sub>4</sub> shows the best cycle performance. The first coulomb efficiency of LiFePO<sub>4</sub> is 87% which is higher than Li(Ni<sub>0.5</sub>Co<sub>0.2</sub>Mn<sub>0.3</sub>)O<sub>2</sub> and LiMn<sub>2</sub>O<sub>4</sub> (84%). The present results also show that the capacity retention rate after 100 cycles of Li(Ni<sub>0.5</sub>Co<sub>0.2</sub>Mn<sub>0.3</sub>)O<sub>2</sub> is 57%, while the capacity retention rate after 100 cycles of LiMn<sub>2</sub>O<sub>4</sub> and LiFePO<sub>4</sub> is higher, 82 and 95%, respectively. Therefore, the cycling stability of Li(Ni<sub>0.5</sub>Co<sub>0.2</sub>Mn<sub>0.3</sub>)O<sub>2</sub> is relatively poor. As shown in **Figure 1B**, the rate performance of LiFePO<sub>4</sub> keeps well at low charge and discharge rate, and the rate performance of Li(Ni<sub>0.5</sub>Co<sub>0.2</sub>Mn<sub>0.3</sub>)O<sub>2</sub> is consistent with cycle performance, but large capacity loss occurs in high rate region. **Figure 1C** presents



the charge-discharge cycle of the three kinds of cathode materials for the first time. The charge-discharge platform of  $\text{LiMn}_2\text{O}_4$  is higher than others. The electrolyte tends to decompose at high charge-discharge platform. Thus, the high charge-discharge platform has an influence on both the electrochemical performance and the safety of the battery. In order to further compare the cycle performance of the three cathode materials at higher temperature, long cycle tests with 0.7 C rate at 55°C were conducted. As shown in **Figure 1D**, the cycle performance of the three kinds of cathodes are obviously influenced and the capacity of  $\text{LiMn}_2\text{O}_4$  drops quickly at the higher temperature, and the  $\text{LiFePO}_4$  still shows a better performance than  $\text{LiMn}_2\text{O}_4$  and  $\text{Li}(\text{Ni}_{0.5}\text{Co}_{0.2}\text{Mn}_{0.3})\text{O}_2$ .

The comparison of the AC impedance resistance and cyclic voltammetry are presented in the **Figure 2**. The results of AC impedance resistance test are shown in **Figure 2A**, according to the formula presented in previous study (Wang et al., 2011), the calculated lithium-ion diffusion coefficients of  $\text{Li}(\text{Ni}_{0.5}\text{Co}_{0.2}\text{Mn}_{0.3})\text{O}_2$ ,  $\text{LiMn}_2\text{O}_4$  and  $\text{LiFePO}_4$  are  $6.85 \times 10^{-9}$ ,  $3.22 \times 10^{-8}$ , and  $2.12 \times 10^{-7}$ , respectively. Thus, the better rate and cycle performance of  $\text{LiFePO}_4$  may attribute from the higher lithium ion diffusion coefficient. **Figures 2B–D** display the cyclic voltammetry of  $\text{Li}(\text{Ni}_{0.5}\text{Co}_{0.2}\text{Mn}_{0.3})\text{O}_2$ ,  $\text{LiMn}_2\text{O}_4$ ,  $\text{LiFePO}_4$ , respectively. Consistent with the charge and discharge curves which are shown in **Figure 1C**, the  $\text{LiFePO}_4$  shows the lowest voltage platform and the best reversibility which contribute to a better cycle performance, while the voltage platforms of  $\text{LiMn}_2\text{O}_4$  and  $\text{Li}(\text{Ni}_{0.5}\text{Co}_{0.2}\text{Mn}_{0.3})\text{O}_2$  are high and the reversibility is not as good as  $\text{LiFePO}_4$ .

### Comparison on Thermal Stability

The variation of weight percent of the charged cathode materials are showed in **Figure 3**. The three materials are stable before around 150°C, thereafter the weight of them decreases at different levels as material decomposition produces gas. In detail,

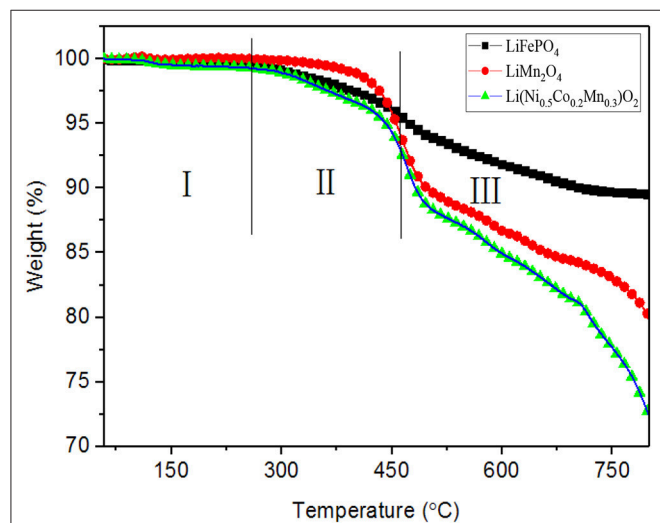


**FIGURE 3** | The weight loss vs. temperature of charged cathode materials.

$\text{LiFePO}_4$  begins to decompose at around 245°C and a total weight loss approaches 10% during the whole process. There are three stages of weight loss for  $\text{LiMn}_2\text{O}_4$ , which are represented by I

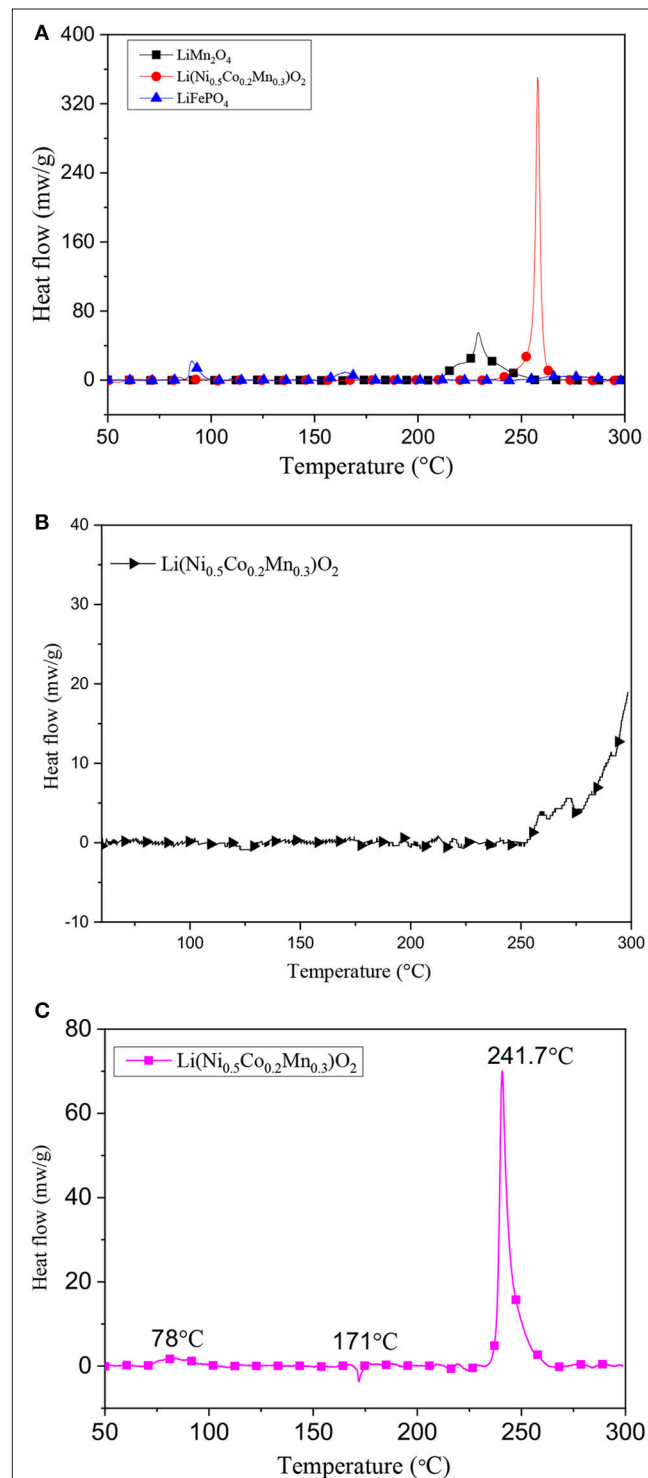
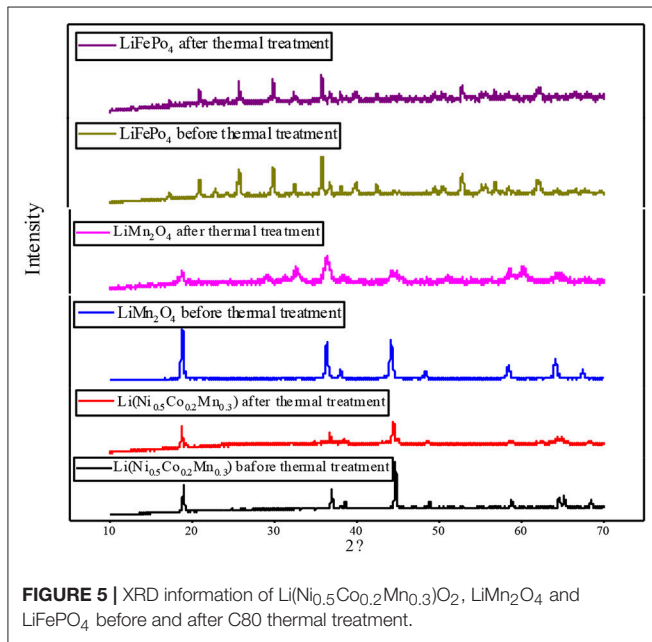
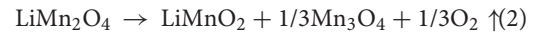
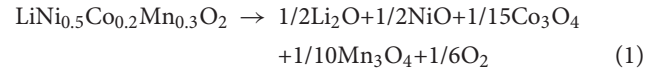


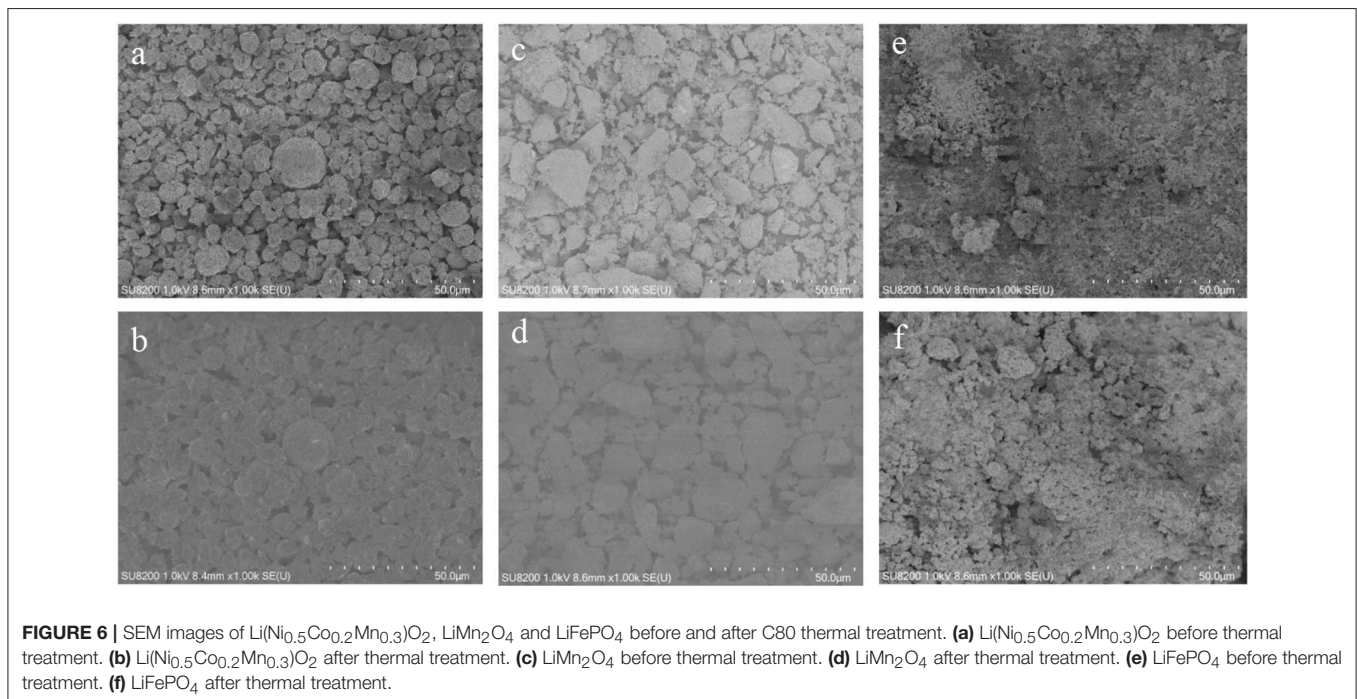
**FIGURE 4** | The heat flow curves of **(A)** the charged cathode materials, and **(B)** pure  $\text{Li}(\text{Ni}_{0.5}\text{Co}_{0.2}\text{Mn}_{0.3})\text{O}_2$ , and **(C)** charged  $\text{Li}(\text{Ni}_{0.5}\text{Co}_{0.2}\text{Mn}_{0.3})\text{O}_2$  - $\text{Li}_4\text{Ti}_5\text{O}_{12}$  full battery.

(before 260°C), II (from 260° to 462°C) and III (after 462°C), respectively. Before 260°C, the weight loss may be attributed to the loss of LiPF<sub>6</sub> or other contaminants. In stage II, PVDF degrades with elimination of hydrogen fluoride in an appreciable quantity along with small amount of C<sub>4</sub>H<sub>3</sub>F<sub>3</sub> (Li et al., 2007). In the stage III, the weight loss is mainly caused by acetylene carbon black and PVDF. As to Li(Ni<sub>0.5</sub>Co<sub>0.2</sub>Mn<sub>0.3</sub>)O<sub>2</sub>, the weight decreases at stage I and drops to almost 71% of original value.

The present results show that LiFePO<sub>4</sub> has better thermal stability than Li(Ni<sub>0.5</sub>Co<sub>0.2</sub>Mn<sub>0.3</sub>)O<sub>2</sub> at high-temperature stage. Based on the data of weight loss and the previous studies (Zaghib et al., 2012; Julien et al., 2014a), LiFePO<sub>4</sub> is stable enough, and the decomposition process of the Li(Ni<sub>0.5</sub>Co<sub>0.2</sub>Mn<sub>0.3</sub>)O<sub>2</sub> and LiMn<sub>2</sub>O<sub>4</sub> can be speculated as follows:



Another thermal experiment was performed by a C80 calorimeter, and the heat flow curves are presented in **Figure 4A**. According to integrate the heat flow, the total heat production of Li(Ni<sub>0.5</sub>Co<sub>0.2</sub>Mn<sub>0.3</sub>)O<sub>2</sub>, LiMn<sub>2</sub>O<sub>4</sub>, LiFePO<sub>4</sub> are −405, −240, and −100 J/g, respectively. In this plot, the exothermic peak of LiFePO<sub>4</sub> around 80 and 160°C may belong to the decomposition of the surface films, but with neglected enough heat production. The decomposition of LiFePO<sub>4</sub> starts to react after 250°C with −38 J/g. While LiMn<sub>2</sub>O<sub>4</sub> and Li(Ni<sub>0.5</sub>Co<sub>0.2</sub>Mn<sub>0.3</sub>)O<sub>2</sub> only have one exothermic peak at 229 and 258°C, respectively. Although the exothermic temperature of LiMn<sub>2</sub>O<sub>4</sub> lowers about 20°C compared with Li(Ni<sub>0.5</sub>Co<sub>0.2</sub>Mn<sub>0.3</sub>)O<sub>2</sub>, the Li(Ni<sub>0.5</sub>Co<sub>0.2</sub>Mn<sub>0.3</sub>)O<sub>2</sub> has a specially sharp exothermic peak with heat generation of −405 J/g. It can be seen that the LiFePO<sub>4</sub> has the best thermal stability among the experimental materials while Li(Ni<sub>0.5</sub>Co<sub>0.2</sub>Mn<sub>0.3</sub>)O<sub>2</sub> has the worst thermal stability among them. As shown in **Figure 4B**, the pure Li(Ni<sub>0.5</sub>Co<sub>0.2</sub>Mn<sub>0.3</sub>)O<sub>2</sub> starts to self-decompose at around 250°C, which is more safer than mixed with the electrolyte. The heat generation of the pure Li(Ni<sub>0.5</sub>Co<sub>0.2</sub>Mn<sub>0.3</sub>)O<sub>2</sub> is totally −88 J/g. The heat flow curve of Li(Ni<sub>0.5</sub>Co<sub>0.2</sub>Mn<sub>0.3</sub>)O<sub>2</sub> −Li<sub>4</sub>Ti<sub>5</sub>O<sub>12</sub>



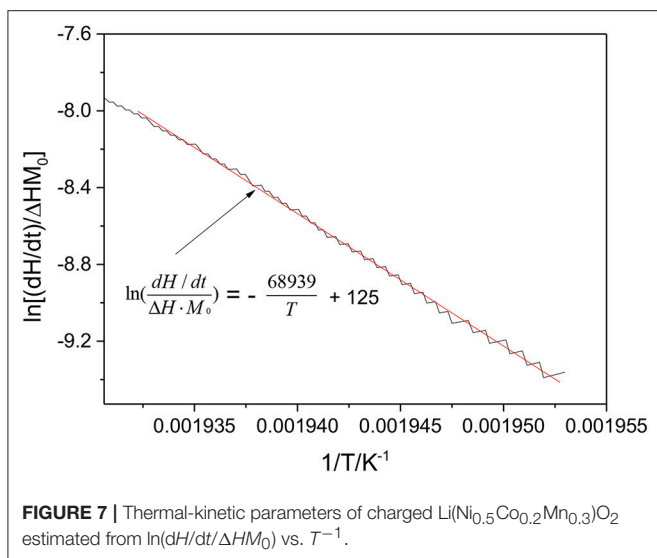


**TABLE 1** | Thermal parameters of different samples at elevated temperature in argon atmosphere.

Samples	Exothermic onset temperature $T_{\text{onset}}(^{\circ}\text{C})$	Reaction heat $\Delta H$ ( $\text{J g}^{-1}$ )	Activation energy $E$ ( $\text{kJ mol}^{-1}$ )	Pre-exponential factor $A$ ( $\text{s}^{-1}$ )
$\text{Li}(\text{Ni}_{0.5}\text{Co}_{0.2}\text{Mn}_{0.3})\text{O}_2$	249	-405	573	$1.93 \times 10^{54}$
$\text{LiMn}_2\text{O}_4$	236	-240	595	$2.32 \times 10^{60}$
$\text{LiFePO}_4$	247	-100	363	$1.01 \times 10^{33}$

full battery is displayed in **Figure 4C**. The total heat generation is  $-810 \text{ J/g}$  with exothermic peak temperature of  $242^{\circ}\text{C}$ . The whole process can be divided into three stages. The first stage belongs to the decomposition of anode material with small heat release at around  $78^{\circ}\text{C}$ . Then the melting of membrane occurs at around  $171^{\circ}\text{C}$  with endothermic reaction due to the heat accumulation in the first stage. Finally, reactions between cathode materials and electrolyte in the third stage generate the most heat in the whole process. Furtherly, in order to better understand the structure changes after thermal treatment of the three cathodes, XRD and SEM tests were carried out to compare the three cathodes materials before and after thermal treatment. **Figure 5** gives the XRD test results, by comparing the result of each sample before and thermal treatment, it can be seen that there is no obvious crystal structure changes of  $\text{LiFePO}_4$  material and the SEM test result in **Figures 6E,F** is almost the same. But for  $\text{Li}(\text{Ni}_{0.5}\text{Co}_{0.2}\text{Mn}_{0.3})\text{O}_2$  and  $\text{LiMn}_2\text{O}_4$  materials, new diffraction peaks appear and some old diffraction peaks disappear, and the crystallinity decreases which all explain that the crystal structure of  $\text{Li}(\text{Ni}_{0.5}\text{Co}_{0.2}\text{Mn}_{0.3})\text{O}_2$  and  $\text{LiMn}_2\text{O}_4$  materials have been destroyed. Furtherly, in **Figures 6A–D**, it presents clearly the change in structures and the appearance of agglomerated particles. These results are consistent with the test results of thermal analysis.

In order to further analyze and compare the thermal stability of the three cathode materials, the chemical kinetic parameters of cathode materials are calculated with C80 data based on the Arrhenius law, which can be written as Wang et al. (2006).

$$\ln\left(\frac{dH/dt}{\Delta HM_0}\right) = -\frac{E}{R} \cdot \frac{1}{T} + \ln A \quad (3)$$

where the  $dH/dt$  is the heat flow,  $\Delta H$  the total heat of reaction,  $M_0$  the initial mass of the reactant,  $E$  the activation energy,  $R$  the gas constant,  $T$  the temperature, and  $A$  the pre-exponential factor. As shown in **Figure 7**, the fitted line of  $\text{Li}(\text{Ni}_{0.5}\text{Co}_{0.2}\text{Mn}_{0.3})\text{O}_2$  were taken as an example by plotting the curve of  $\ln(dH/dt/\Delta HM_0)$  vs. inverse temperature ( $1/T$ ). The activation energy of  $\text{Li}(\text{Ni}_{0.5}\text{Co}_{0.2}\text{Mn}_{0.3})\text{O}_2$ -electrolyte system is  $539 \text{ kJ/mol}$ , and the pre-exponential factor is  $7.48 \times 10^{53} \text{ s}^{-1}$ . The thermal kinetic parameters for other experimental materials are listed in **Table 1** by the same method. The results show that  $\text{LiFePO}_4$  has the minimum activation energy for the sake of the decomposition of surface films. However, it is unsuitable to choose the activation energy to judge the thermal stability of  $\text{LiFePO}_4$  as this parameter is not calculated according to the decomposition of the material itself.

## CONCLUSIONS

The comparison of electrochemical performance and thermal stability among charged  $\text{Li}(\text{Ni}_{0.5}\text{Co}_{0.2}\text{Mn}_{0.3})\text{O}_2$ ,  $\text{LiMn}_2\text{O}_4$ , and  $\text{LiFePO}_4$  were investigated in this paper. With the help of charge-discharge cycling and impedance measurement, it can be seen that cycle performance of  $\text{Li}(\text{Ni}_{0.5}\text{Co}_{0.2}\text{Mn}_{0.3})\text{O}_2$  is not as stable as  $\text{LiMn}_2\text{O}_4$  and  $\text{LiFePO}_4$ . Furthermore, the comparison and analysis of thermal stability is conducted by the thermogravimetric (TG) instrument and C80 instrument. The present results show that  $\text{LiFePO}_4$  has the best thermal stability with the heat generation of  $-100 \text{ J/g}$  among the tested materials, whereas  $\text{Li}(\text{Ni}_{0.5}\text{Co}_{0.2}\text{Mn}_{0.3})\text{O}_2$  produces the heat of  $-405 \text{ J/g}$ . Finally, the thermal stability of these materials is further evaluated by calculating the thermal kinetic parameters based on the Arrhenius law. The present results reveal that  $\text{Li}(\text{Ni}_{0.5}\text{Co}_{0.2}\text{Mn}_{0.3})\text{O}_2$  full battery has a high risk of thermal runaway.

## AUTHOR CONTRIBUTIONS

All authors listed have made a substantial, direct and intellectual contribution to the work, and approved it for publication.

## ACKNOWLEDGMENTS

This work is supported by the Science and Technology Project from China Southern Power Grid (No. GDKJQQ20152008).

## REFERENCES

- Chen, L., Guo, X., Lu, W., Chen, M., Li, Q., Xue, H., et al. (2018). Manganese monoxide-based materials for advanced batteries. *Coordinat. Chem. Rev.* 368, 13–34. doi: 10.1016/j.ccr.2018.04.015
- Chen, Y.-B., Hu, Y., Lian, F., and Liu, Q.-G. (2010). Synthesis and characterization of spinel  $\text{Li}_{1.05}\text{Cr}_{0.1}\text{Mn}_{1.9}\text{O}_{4-z}\text{F}_z$  as cathode materials for lithium-ion batteries. *Int. J. Min. Metal. Mater.* 17, 220–224. doi: 10.1007/s12613-010-0217-8
- Du, Y., Huang, X., Zhang, K., Liang, F., Li, Q., Yao, Y., et al. (2016). Thermal stability of  $\text{LiFePO}_4/\text{C}-\text{LiMn}_2\text{O}_4$  blended cathode materials. *Sci. China Technol. Sci.* 60, 58–64. doi: 10.1007/s11431-016-0329-7
- Feng, C., Li, H., Zhang, P., Guo, Z., and Liu, H. (2010). Synthesis and modification of non-stoichiometric spinel ( $\text{Li}_{1.02}\text{Mn}_{1.90}\text{Y}_{0.02}\text{O}_{4-y}\text{F}_{0.08}$ ) for lithium-ion batteries. *Mater. Chem. Phys.* 119, 82–85. doi: 10.1016/j.matchemphys.2009.07.049
- Gong, J., Wang, Q., and Sun, J. (2017). Thermal analysis of nickel cobalt lithium manganese with varying nickel content used for lithium ion batteries. *Thermochim. Acta* 655, 176–180. doi: 10.1016/j.tca.2017.06.022
- Hannan, M.A., Lipu, M.S.H., Hussain, A., and Mohamed, A. (2017). A review of lithium-ion battery state of charge estimation and management system in electric vehicle applications: challenges and recommendations. *Renew. Sustain. Energy Rev.* 78, 834–854. doi: 10.1016/j.rser.2017.05.001
- Julien, C.M., Mauger, A., Grout, H., and Zaghib, K. (2014a). Surface modification of positive electrode materials for lithium-ion batteries. *Thin Solid Films* 572, 200–207. doi: 10.1016/j.tsf.2014.07.063
- Julien, C.M., Mauger, A., Zaghib, K., and Grout, H. (2014b). Comparative issues of cathode materials for Li-ion batteries. *Inorganics* 2, 132–154. doi: 10.3390/inorganics2010132
- Li, L., Zhu, Z.H., Yan, Z.F., Lu, G.Q., and Rintoul, L. (2007). Catalytic ammonia decomposition over Ru/carbon catalysts: the importance of the structure of carbon support. *Appl. Catalysis A Gen.* 320, 166–172. doi: 10.1016/j.apcata.2007.01.029
- Lu, Y., Li, B., Zheng, S., Xu, Y., Xue, H., and Pang, H. (2017). Syntheses and energy storage applications of  $\text{M}_x\text{S}_y$  ( $M = \text{Cu}, \text{Ag}, \text{Au}$ ) and their composites: rechargeable batteries and supercapacitors. *Adv. Funct. Mater.* 27:1703949. doi: 10.1002/adfm.201703949
- Luo, W., and Zheng, B. (2017). Improved electrochemical performance of  $\text{LiNi}_{0.5}\text{Co}_{0.2}\text{Mn}_{0.3}\text{O}_2$  cathode material by double-layer coating with graphene oxide and  $\text{V}_2\text{O}_5$  for lithium-ion batteries. *Appl. Surface Sci.* 404, 310–317. doi: 10.1016/j.apsusc.2017.01.200
- Ma, J., Guo, X., Yan, Y., Xue, H., and Pang, H. (2018).  $\text{FeO}_x$ -based materials for electrochemical energy storage. *Adv. Sci. (Weinh.)* 5:1700986. doi: 10.1002/advs.201700986
- Ouyang, C.Y., Shi, S.Q., and Lei, M.S. (2009). Jahn–Teller distortion and electronic structure of  $\text{LiMn}_2\text{O}_4$ . *J. Alloys Compounds* 474, 370–374. doi: 10.1016/j.jallcom.2008.06.123
- Sun, Y.K., Myung, S.T., Park, B.C., Prakash, J., Belharouak, I., and Amine, K. (2009). High-energy cathode material for long-life and safe lithium batteries. *Nat. Mater.* 8, 320–324. doi: 10.1038/nmat2418
- Susanto, D., Kim, H., Kim, J.-Y., Lim, S., Yang, J., Choi, S.A., et al. (2015). Effect of (Mg, Al) double doping on the thermal decomposition of  $\text{LiMn}_2\text{O}_4$  cathodes investigated by time-resolved X-ray diffraction. *Curr. Appl. Phys.* 15, S27–S31. doi: 10.1016/j.cap.2015.01.027
- Wang, Q., Ping, P., Zhao, X., Chu, G., Sun, J., and Chen, C. (2012). Thermal runaway caused fire and explosion of lithium ion battery. *J. Power Sources* 208, 210–224. doi: 10.1016/j.jpowsour.2012.02.038
- Wang, Q., Sun, J., Yao, X., and Chen, C. (2006). Micro calorimeter study on the thermal stability of lithium-ion battery electrolytes. *J. Loss Prevent. Process Ind.* 19, 561–569. doi: 10.1016/j.jlp.2006.02.002
- Wang, X., Hao, H., Liu, J., Huang, T., and Yu, A. (2011). A novel method for preparation of macroporous lithium nickel manganese oxygen as cathode material for lithium ion batteries. *Electrochim. Acta* 56, 4065–4069. doi: 10.1016/j.electacta.2010.12.108
- Xu, W., Yuan, A., Tian, L., and Wang, Y. (2011). Improved high-rate cyclability of sol-gel derived Cr-doped spinel  $\text{LiCr}_y\text{Mn}_{2-y}\text{O}_4$  in an aqueous electrolyte. *J. Appl. Electrochem.* 41, 453–460. doi: 10.1007/s10800-011-0255-6
- Yang, K., Fan, L.-Z., Guo, J., and Qu, X. (2012). Significant improvement of electrochemical properties of  $\text{AlF}_3$ -coated  $\text{LiNi}_{0.5}\text{Co}_{0.2}\text{Mn}_{0.3}\text{O}_2$  cathode materials. *Electrochim. Acta* 63, 363–368. doi: 10.1016/j.electacta.2011.12.121
- Yi, T.-F., Yin, L.-C., Ma, Y.-Q., Shen, H.-Y., Zhu, Y.-R., and Zhu, R.-S. (2013). Lithium-ion insertion kinetics of Nb-doped  $\text{LiMn}_2\text{O}_4$  positive-electrode material. *Ceramics Int.* 39, 4673–4678. doi: 10.1016/j.ceramint.2012.10.256
- Zaghib, K., Dubé, J., Dallaire, A., Galoustov, K., Guerfi, A., Ramanathan, M., et al. (2012). Enhanced thermal safety and high power performance of carbon-coated  $\text{LiFePO}_4$  olivine cathode for Li-ion batteries. *J. Power Sources* 219, 36–44. doi: 10.1016/j.jpowsour.2012.05.018

**Conflict of Interest Statement:** GZ, CW, and KX were employed by company Electric Power Research Institute of Guangdong Power Grid Co., Ltd.

The remaining authors declare that the research was conducted in the absence of any commercial or financial relationships that could be construed as a potential conflict of interest.

Copyright © 2018 Zhong, Gong, Wang, Xu and Chen. This is an open-access article distributed under the terms of the Creative Commons Attribution License (CC BY). The use, distribution or reproduction in other forums is permitted, provided the original author(s) and the copyright owner(s) are credited and that the original publication in this journal is cited, in accordance with accepted academic practice. No use, distribution or reproduction is permitted which does not comply with these terms.